Molecular Biology of the Cell
Vol. 17, 1514–1526, April 2006

Rab1 Defines a Novel Pathway Connecting the Pre-Golgi Intermediate Compartment with the Cell Periphery[V]

Ragna Sannerud,*† Michaël Marie,* Clément Nizak,‡§ Hege Avsnes Dale,‖ Karin Pernet-Gallay,‡ Franck Perez,‡ Bruno Goud,‡ and Jaakko Saraste*

*Section of Anatomy and Cell Biology and ‖Molecular Imaging Center, Department of Biomedicine, University of Bergen, N-5009 Bergen, Norway; and ‡Centre National de la Recherche Scientifique Unité Mixte de Recherche 144, Institut Curie, Section de Recherche, 75248 Paris Cedex 05, France

Submitted August 25, 2005; Revised December 21, 2005; Accepted January 5, 2006
Monitoring Editor: Jennifer Lippincott-Schwartz

The function of the pre-Golgi intermediate compartment (IC) and its relationship with the endoplasmic reticulum (ER) and Golgi remain only partially understood. Here, we report striking segregation of IC domains in polarized PC12 cells that develop neurite-like processes. Differentiation involves expansion of the IC and movement of Rab1-containing tubules to the growth cones of the neurites, whereas p58- and COPI-positive IC elements, like rough ER and Golgi, remain in the cell body. Exclusion of Rab1 effectors p115 and GM130 from the neurites further indicated that the centrifugal, Rab1-mediated pathway has functions that are not directly related to ER-to-Golgi trafficking. Disassembly of COPI coats did not affect this pathway but resulted in missorting of p58 to the neurites. Live cell imaging showed that green fluorescent protein (GFP)–Rab1A-containing IC elements move bidirectionally both within the neurites and cell bodies, interconnecting different ER exit sites and the *cis*-Golgi region. Moreover, in nonpolarized cells GFP-Rab1A-positive tubules moved centrifugally towards the cell cortex. Hydroxymethylglutaryl-CoA reductase, the key enzyme of cholesterol biosynthesis, colocalized with slowly sedimenting, Rab1-enriched membranes when the IC subdomains were separated by velocity sedimentation. These results reveal a novel pathway directly connecting the IC with the cell periphery and suggest that this Rab1-mediated pathway is linked to the dynamics of smooth ER.

INTRODUCTION

The secretory apparatus of eukaryotic cells consists of a series of membrane-bound compartments connected by bidirectional transport pathways. The best characterized organelles of this system, the endoplasmic reticulum (ER) and the Golgi apparatus, are dynamic structures that can change their size and shape depending on external signals and cellular needs (Nunnari and Walter, 1996). Growth and reorganization of these organelles are required for their accurate partitioning during cell division (Warren and Wickner, 1996). In addition, both are composed of distinct subcompartments, and functional specialization of different cell types is often accompanied by proliferation of these subdomains (Pfeffer, 2003). For example, cells that are active in protein secretion (such as plasma cells and pancreatic exocrine cells) contain massive amounts of ribosome-coated rough ER (RER), whereas neurons, muscle cells, and steroidogenic cells develop extensive smooth ER (SER) networks specialized in cholesterol and lipid biosynthesis and intracellular calcium signaling (Vertel *et al*., 1992; Baumann and Walz, 2001). How cells regulate the biogenesis of these secretory organelles and their subdomains is not well understood. However, the control mechanisms are likely to be related to signaling pathways that coordinate the synthesis of organelle proteins and lipids and may involve membrane traffic between the ER and Golgi (Wiest *et al*., 1990; Cox *et al*., 1997; Nohturfft *et al*., 2000; van Anken *et al*., 2003).

Transport of proteins between the ER and the Golgi apparatus is mediated by pre-Golgi structures that are frequently referred to as vesicular-tubular clusters (VTCs) or collectively as the intermediate compartment (IC or ERGIC) (Saraste and Kuismanen, 1992; Hauri *et al*., 2000; Klumperman, 2000; Lippincott-Schwartz *et al*., 2000). It still remains unclear whether the pleiomorphic IC elements are simply transport carriers or constitute a functionally more complex membrane system. They form at ER exit sites (ERES), stationary, COPII-coated structures scattered throughout the ER network (Hammond and Glick, 2000; Stephens *et al*., 2000; Tang *et al*., 2000) via a protrusion or fusion process (Antonny and Schekman, 2001; Mironov *et al*., 2003) that is linked to microtubule dynamics (Watson *et al*., 2005). Subsequently, they move in a microtubule-dependent manner to the *cis*-Golgi region (Saraste and Svensson, 1991; Mizuno and Singer, 1994; Presley *et al*., 1997; Scales *et al*., 1997) or interact with *cis*-Golgi elements via tubulo-vesicular carriers (Ben-Tekaya *et al*., 2005). The IC elements can change their composition by recycling membrane components (Martinez-Menarguez *et al*., 1999) and receiving material from the Golgi apparatus (Marra *et al*., 2001) and develop membrane

This article was published online ahead of print in *MBC in Press* (http://www.molbiolcell.org/cgi/doi/10.1091/mbc.E05–08–0792) on January 18, 2006.

[V] The online version of this article contains supplemental material at *MBC Online* (http://www.molbiolcell.org).

Present addresses: † Laboratory for Membrane Trafficking, Center for Human Genetics, Gasthuisberg, KULeuven/VIB4, B-3000 Leuven, Belgium; § Rockefeller University, Center for Studies in Physics and Biology, Living Matter Laboratory, Box 34, 1230 York Avenue, New York, NY 10021.

Address correspondence to: Jaakko Saraste (jaakko.saraste@biomed.uib.no).

© 2006 by The American Society for Cell Biology

domains that may have specific functions in bidirectional ER–Golgi trafficking (Saraste and Kuismanen, 1984; Tang *et al*., 1995; Martinez-Menarguez *et al*., 1999; Shima *et al*., 1999; Horstmann *et al*., 2002). Interestingly, the IC expands in transport-arrested cells (Kuismanen and Saraste, 1989; Trucco *et al*., 2004) but also in response to accumulation of unfolded proteins (Raposo *et al*., 1995; Zuber *et al*., 2004), and it is prominent in professional secretory cells (Lahtinen *et al*., 1992; Sesso *et al*., 1994; Martinez-Menarguez *et al*., 1999), suggesting that cells can modulate the size and function of this compartment.

Rab1 is a GTPase that predominantly localizes to the IC membranes (Griffiths *et al*., 1994; Saraste *et al*., 1995; Sannerud, Berger Hansen, and Saraste, unpublished data). It is present in cells as two isoforms, Rab1A and Rab1B, which both have been suggested to regulate anterograde transport of cargo between the ER and the Golgi apparatus (Plutner *et al*., 1991; Tisdale *et al*., 1992). However, in addition to globular elements enriched in anterograde cargo, Rab1 also associates with IC tubules that accumulate in transport-arrested cells and are devoid of cargo proteins (Palokangas *et al*., 1998). These findings raised the possibility that Rab1 (or one of its isoforms) functions in a retrograde transport process at the ER–Golgi boundary (Palokangas *et al*., 1998; Sannerud *et al*., 2003).

Here, we have used Rab1 and p58, the rat ortholog of the human cargo receptor ERGIC-53 (Lahtinen *et al*., 1992; Hauri *et al*., 2000), to examine the distribution and dynamics of the IC in neuroendocrine PC12 cells, a commonly used model to study neuronal differentiation (Greene and Tischler, 1976). When treated with nerve growth factor (NGF), these cells reorganize their endomembranes and develop long, neuritelike processes, resulting in massive increase in the plasma membrane area (Luckenbill-Edds *et al*., 1979). However, the intracellular transport routes that support cell polarization and plasma membrane expansion during neurite outgrowth remain largely unknown (Futerman and Banker, 1996; Valtorta and Leoni, 1999). We show here that Rab1-containing IC elements and ERES are selectively redistributed to the neurites and growth cones of polarized PC12 cells, providing evidence for a Golgi-bypass pathway that functions in the delivery of membranes to the developing neurites. Imaging of green fluorescent protein (GFP)-Rab1A dynamics in living HeLa and normal rat kidney (NRK) cells further showed that a similar centrifugal route also operates in nonpolarized cells. Based on compositional properties of the Rab1-containing IC tubules, we propose that this pathway is linked to the dynamics of SER and functions in cholesterol transport from the early secretory route to cortical regions of the cell.

MATERIALS AND METHODS

Antibodies and Reagents

The rabbit antibody detecting both isoforms of Rab1 (Saraste et al., 1995) was affinity-purified using the glutathione *S*-transferase (GST)-Rab1A fusion protein. Affinity purification of rabbit anti-p58 has been described previously (Saraste and Svensson, 1991). Rabbit anti-synaptophysin was purchased from Synaptic Systems (Göttingen, Germany), anti-hydroxymethylglutaryl (HMG)-CoA reductase was from Upstate Biotechnology (Lake Placid, NY), and anti-BiP was from Stressgen Biotechnologies (Victoria, British Columbia, Canada). The polyclonal anti-Rab1B and anti-β-COP were from Santa Cruz Biotechnology (Santa Cruz, CA) and Affinity Bioreagents (Golden, CO), respectively. The other primary antibodies were generous gifts from the following sources: affinity-purified rabbit anti-mSec13 and monoclonal anti-Sec31a were from Bor Luen Tang and Wanjin Hong (University of Singapore, Singapore), rabbit anti-SPC25 was from Stephen High (University of Manchester, Manchester, United Kingdom), mouse anti-ribophorin I was from Gert Kreibich (New York University, New York, NY), rabbit anti-mannosidase II was from Kelley Moremen (University of Georgia, Athens, GA), rabbit anti-GM130 was from Nobuhiro Nakamura (Kanazawa University, Kanazawa City, Japan); affinity-purified rabbit anti-α-TRAP was from Tom Rapoport (Harvard University, Cambridge, MA); rabbit anti-p115 was from Elizabeth Sztul (University of Alabama, Birmingham, AL), and mouse anti-β'-COP was from Felix Wieland (Biochemie-Zentrum, Heidelberg, Germany). Fluorescent secondary antibodies and 6-[*N*-(7-nitrobenz-2-oxa-1,3-diazole-4-yl)amino]-hexanoyl-D-*erythro*-sphingosine] (NBD-ceramide) were purchased from Jackson ImmunoResearch Laboratories (West Grove, PA) and Molecular Probes (Eugene, OR) respectively. The mounting medium was from Vector Laboratories (Burlingame, CA).

Construction of Fluorescent Fusion Proteins

A DNA fragment encoding the full-length sequence of dog Rab1A (GenBank accession no. X56384) was generated by BamHI digestion of the pGEX-Rab1A vector (kindly provided by Tommy Nilsson, University of Gothenburg, Gothenburg, Sweden). This BamHI/BamHI DNA fragment was inserted into the BglII/BamHI-digested pEGFP-C1 vector (GenBank accession no. U55763; Clontech, Mountain View, CA) to generate pEGFP-Rab1A. Correct insertion of the generated vector was confirmed by sequencing. The linker between GFP and Rab1A consisted of six amino acids (Ser-Gly-Leu-Arg-Ser-Ala). The yellow fluorescent protein-p58 construct (YFP-p58P) was generated by inserting YFP at the proline-rich region between the CRD and stalk domains of p58 (Lahtinen *et al*., 1996; Matti Saraste, personal communication). Two DNA fragments, corresponding to base pairs 11-838 (1) and 839-1564 (2) of rat p58 cDNA (Lahtinen *et al*., 1996; GenBank accession no. U44129) were prepared by PCR using the primers 5′-ATC GCT AGC GAT GGC GGT GTC CAG GCG-3′ and 5′-TTG ACC GGT CCG GTT AGT TGG AAA GTC AG-3′ (1) and 5′-CTC AAG CTT CGG AGC CCG GAA AAG AGC C-3′ and 5′-GAG GAT CCT CAG AAG AAT TTT TTG GCA GC-3′ (2). The PCR products were inserted at the 5′ and 3′ ends of the YFP coding sequence in the pEYFP-C1 expression vector (Clontech), respectively, and the accuracy of final constructs were confirmed by sequencing.

Cell Culture, Transfection, and Drug Treatments

These experiments used both the original PC12 cell line (ATCC CRL-1721), and a subclone derived from it (kindly provided Eivind Rødahl, Haukeland Hospital, Bergen, Norway). Attachment of the former requires pretreatment of the culture dishes with rat tail collagen type I (Upstate Biotechnology), whereas the latter adheres without precoating and shows homogenous response to NGF. Similar results were obtained with both cell types. The cultivation of PC12, HeLa, and NRK cells has been described previously (Palokangas *et al*., 1998). NGF (2.5S) was purchased from Invitrogen (Carlsbad, CA) and added to the complete PC12 cell growth medium at 20 ng/ml. Transfections using LipofectAMINE 2000 (Invitrogen) were performed according to the manufacturer's instructions. Brefeldin A (Epicenter Technologies, Madison, WI) was added to the medium at 5 μg/ml from 1000× ethanol stock solution kept at −20°C. Nocodazole (Sigma-Aldrich, St. Louis, MO), stored as 10 mM dimethyl sulfoxide stock solution at −20°C, was used at the final concentration of 10 μM.

Cell Fractionation

Velocity sedimentation of 3000 × *g* supernatants prepared from PC12 cells was carried out as described in detail previously (Majoul *et al*., 1996; Sannerud, Berger Hansen, and Saraste, unpublished data). Briefly, PC12 cells grown in 75-cm^2 culture flasks were washed successively with Hank's balanced salt solution (Invitrogen), phosphate-buffered saline, and 140 mM NaCl, 30 mM KCl, 10 mM EDTA, 25 mM Tris-HCl, pH 7.4. Cell pellets were resuspended in 0.75 ml of 130 mM KCl, 25 mM NaCl, 1 mM EGTA, 25 mM Tris-HCl, pH 7.4 (homogenization solution; HS), supplemented with protease inhibitors (Complete Mini; Boehringer, Mannheim, Germany), and homogenized by 30 ↔ passages through a ball-bearing cell cracker (European Molecular Biology Laboratory, Heidelberg, Germany) with the clearance set at 10 μm. Nuclei were removed by centrifugation for 10 min at 600 × *g*, where after the postnuclear supernatants were centrifuged for 10 min at 3000 × *g*. Samples of the supernatants (0.5 ml) were layered on top of iodixanol (OptiPrep, Axis-Schield) step gradients prepared in SW41 UltraClear tubes (from top to bottom, 1.2 ml each of 5, 7.5, 10, 12.5, 15, 17.5, 20, 22.5, and 25% iodixanol in HS). After centrifugation in Beckman LE-80K ultracentrifuge for 30 min at 126.000 × *g*, 11 fractions (2–8 corresponding to visible membrane bands) were collected from the top, diluted with HS, and membranes were concentrated by centrifugation for 90 min at 100,000 × *g*. They were resuspended in HS supplemented with Complete Mini and 10 μg/ml each of chymostatin, leupeptin, antipain, and pepstatin (Sigma-Aldrich), and frozen in aliquots at −20°C.

Gel Electrophoresis and Immunoblotting

Aliquots of the resuspended membrane pellets were mixed with concentrated sample buffer. The proteins were separated by SDS-PAGE using 12% polyacrylamide gels, and transferred to nitrocellulose membranes, which were typically cut into horizontal strips with the help of 10- to 250-kDa prestained markers (Bio-Rad, Hercules, CA) and staining with Ponceau S. The strips were first incubated 2 h to overnight in 20 mM Tris-HCl, pH 7.5, 150 NaCl, 0.1% Tween 20, and 5% nonfat dry milk (blocking buffer; BB), followed by 2-h

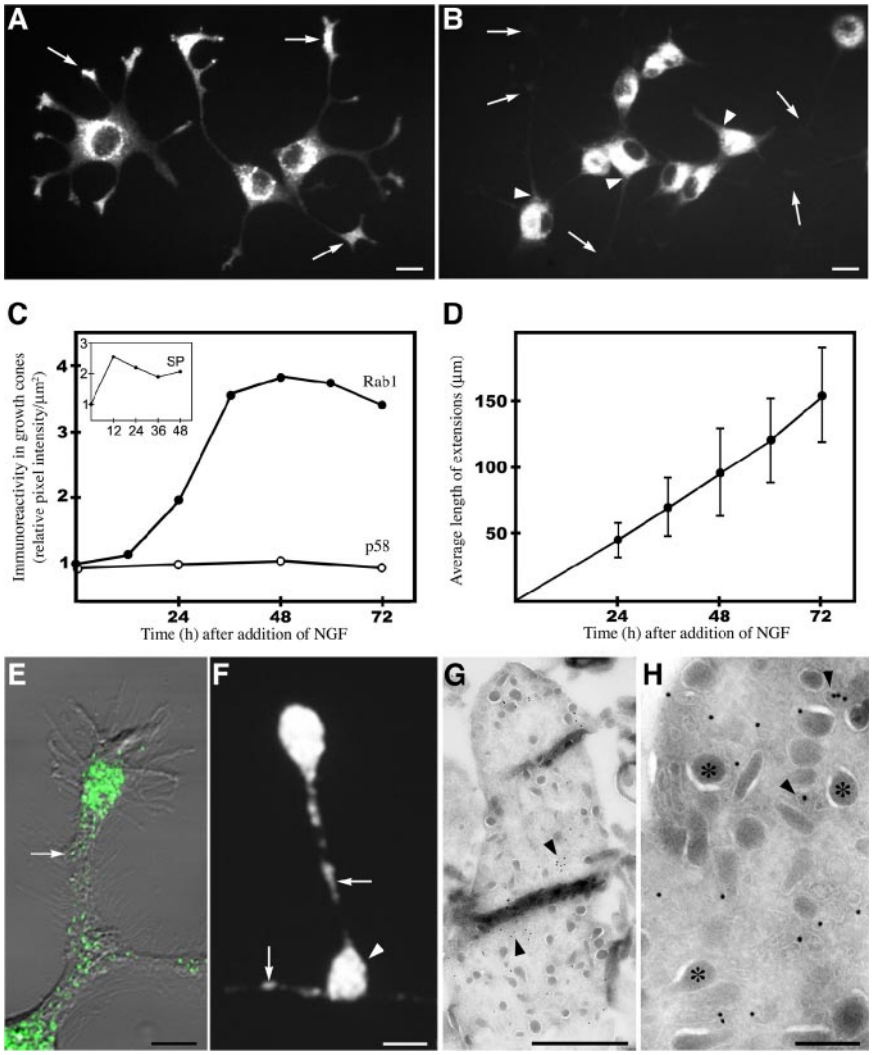

Figure 1. Segregation of Rab1 and p58 in polarized PC12 cells. (A and B) Differentiating PC12 cells (48-h NGF) were stained for endogenous Rab1 (A) or p58 (B). Note accumulation of Rab1 in the growth cones (A, arrows) and exclusion of p58 from the neurites (B). Arrowheads indicate neck regions of the neurites. (C) Kinetics of appearance of Rab1 in the growth cones. For comparison, the inset shows the kinetics of transport of synaptophysin (SP) to these sites. (D) Linear growth of neurites during the NGF treatment. (E and F) Rab1-positive elements within the neurites (arrows) accumulate at the varicosities (F, arrowhead) and throughout the growth cones. (G and H): Immunoelectron microscopy shows the association of Rab1 with pleiomorphic, smooth membrane structures within the growth cones (arrowheads). Asterisks indicate secretory granules that are not labeled. Bars, 10 μm (A and B), 5 μm (F), 1 μm (G), and 0.2 μm (H).

incubation with primary antibodies (diluted in BB), extensive washing, and 1-h staining with horseradish peroxidase-coupled anti-rabbit IgG (Jackson ImmunoResearch Laboratories; diluted in BB). After final washing, the chemiluminescence reaction (Super Signal; Pierce Chemical, Rockford, IL) was carried out, and immunoreactive protein bands were visualized and quantitated using Fuji LAS 3000 imager.

Immunofluorescence Staining and Confocal Microscopy

The processing of cells for immunofluorescence microscopy has been described previously (Palokangas *et al*., 1998). For staining with anti-ribophorin I and anti-SPC25, the cells were treated with 6 M guanidine-HCl to expose antigenic sites (Ying *et al*., 2002). Confocal imaging was performed using either Leica TCS SP2 AOBS or Zeiss LSM 510 Meta confocal laser scanning microscopes. Optical sections were obtained using either 63× (numerical aperture [NA] 1.4–1.45) or 100× (NA 1.4) oil immersion objectives. The fluorescent signals in the growth cones were quantitated using the standard Leica software. Regions of interests were defined and their relative fluorescence intensities (arbitrary units per square micrometer) were calculated based on the total pixel intensities and surface areas. The background signal was determined for growth cones of cells reacted only with secondary antibodies and subtracted from the values. For each time point, the fluorescence intensities of 40–60 growth cones, set within the dynamic range of measurement, were determined from two separate experiments.

Live Cell Imaging

For imaging of the fluorescent proteins in living cells, the transfected cells on coverslips were placed in a 37°C incubation chambers, attached to either Leica SP2 or Zeiss Axiovert 200 microscopes, and filled with phenol red-free culture medium buffered at pH 7.5 with 20 mM HEPES. Time-lapse confocal microscopy of GFP-Rab1A was carried out using Leica SP2 equipped with a 63× oil immersion objective (1.4 NA), at a definition of 512 × 512 pixels, and with the pinhole set at 1 airy disk. GFP was excited with a 488-nm laser line and imaged with a 505- to 560-nm band-pass filter. Data were processed using the ImageJ software (available at http://rsb.info.nih.gov/ij/) and Adobe ImageReady 7.0 (Adobe Systems, Mountain View, CA. The final figures were prepared using Adobe Photoshop 7. The fluorescence intensity profiles and SD projections were obtained using the ImageJ software. Spinning disk confocal microscopy of HeLa and NRK cells expressing GFP-Rab1A or YFP-p58 was performed using the Ultraview RS Live Cell Imager (PerkinElmer Life and Analytical Sciences, Boston, MA). The cells were viewed with 63×/1.4 NA Plan-Apochromat oil immersion objective, and images were acquired with an Argon laser. Z-stacks of the entire cell depth were acquired for each time point. The images were processed using Volocity (Improvision, Lexington, MA) and the NIH ImageJ software.

Immunoelectron Microscopy

Cells were fixed for 30 min with 2% paraformaldehyde (PFA), 0.125% glutaraldehyde and then for 2 h with 2% PFA. They were processed for cryosectioning as described previously (Raposo *et al*., 1997). Cryosections were obtained using Leica Ultracut FCS ultracryomicrotome, retrieved with a 1:1 solution of 2.3 M sucrose and 2% methylcellulose, and incubated with affinity-purified anti-Rab1, followed by 15-nm protein A-gold (Department of Cell Biology, University of Utrecht, Utrecht, The Netherlands). The immunolabeled sections were viewed at 80 kV in a Philips CM120 electron microscope.

RESULTS

Segregation of Rab1 and p58 in Polarized PC12 Cells

Because the differentiation of PC12 cells has been previously shown to involve structural and functional changes of the

Golgi complex (Luckenbill-Edds *et al*., 1979; Hickey *et al*., 1983), it was of interest to examine whether the organization of the IC is also affected. We first studied the localization of Rab1 and p58 in control PC12 cells and at different times after addition of NGF. Previous studies suggested that the two IC proteins have largely overlapping distributions (Krijnse-Locker *et al*., 1995; Saraste *et al*., 1995), and their localizations in control PC12 cells were also similar (Figure 3, A and B, insets). However, they displayed strikingly different distributions in the NGF-treated PC12 cells. Whereas p58 was restricted to the cell bodies, Rab1 was also present in the neurites, being predominantly enriched in the growth cones (Figure 1, A and B). The Rab1-positive IC elements were evenly distributed throughout the growth cones, but they were absent from filopodia (Figure 1E). They were also detected along the neurites, concentrating in their varicosities (Figure 1, E and F). Similar, partial segregation of Rab1 and p58 was observed in cultured hippocampal neurons (Sannerud and Saraste, unpublished data). Results obtained with GFP-Rab1A (Figure 7), and using antibodies against endogenous Rab1B (our unpublished data), indicated that both Rab1 isoforms are present in the neurites.

Determination of the kinetics of redistribution of Rab1 to the growth cones showed that the Rab1-specific signal started to increase at ~12 h, reaching a plateau at ~36 h after NGF addition (Figure 1C). At the same time, the p58 signal in the growth cones did not increase (Figure 1C). In contrast to Rab1, synaptophysin, an integral membrane protein of synapticlike microvesicles that follows the constitutive post-Golgi pathway (Kelly and Grote, 1993) was transported to the growth cones within the first 12 h after addition of NGF (Figure 1C, inset). Also, because the length of the neurites increased linearly during the first 72 h of NGF treatment (Figure 1D), we conclude that the redistribution of Rab1 to the neurites is a regulated process that depends on their maturation.

Rab1 Associates with Pleiomorphic Structures in the Growth Cones

The growth cones of NGF-treated PC12 cells can be easily identified in the electron microscope because of their characteristic shape and the presence of numerous secretory granules (Luckenbill-Edds *et al*., 1979) (Figure 1G). In accordance with the confocal microscopic results (Figure 1, E and F), immunogold labeling of cryosections showed that the Rab1-containing IC elements are present throughout the growth cones. They seemed to be highly heterogenous in size and shape, including both small tubulo-vesicular and larger pleiomorphic structures (Figure 1, G and H). Within the cell bodies Rab1 associated with membranes at the *cis*-face of the Golgi apparatus as well as peripheral tubulovesicular and vacuolar IC elements (our unpublished data), as described previously in other cell types (Griffiths *et al*., 1994; Saraste *et al*., 1995).

RER, Golgi, and Rab1 Effectors, but Not ERES, Are Excluded from the Neurites

To study the topology of early secretory compartments in the NGF-treated PC12 cells, we first examined the localization of RER and Golgi markers by confocal microscopy. Ribophorin I, a subunit of oligosaccharyl transferase (Wilson *et al*., 2005), was mainly restricted to the cell bodies (Figure 2A), but it frequently extended to the neck regions of the neurites. Localization of the signal peptidase subunit SPC25, and the translocon component αTRAP (Baumann and Walz, 2001), gave similar results (our unpublished data). Golgi membranes were also restricted to the cell bodies, as shown by localization of mannosidase II (Figure 2B), and the fluorescent lipid analog NBD-ceramide, markers of *cis*-medial and *trans*-Golgi cisternae, respectively. The two tethering factors, p115 and GM130, that functionally interact with Rab1 (Allan *et al*., 2000; Moyer *et al*., 2001; Weide *et al*., 2001;

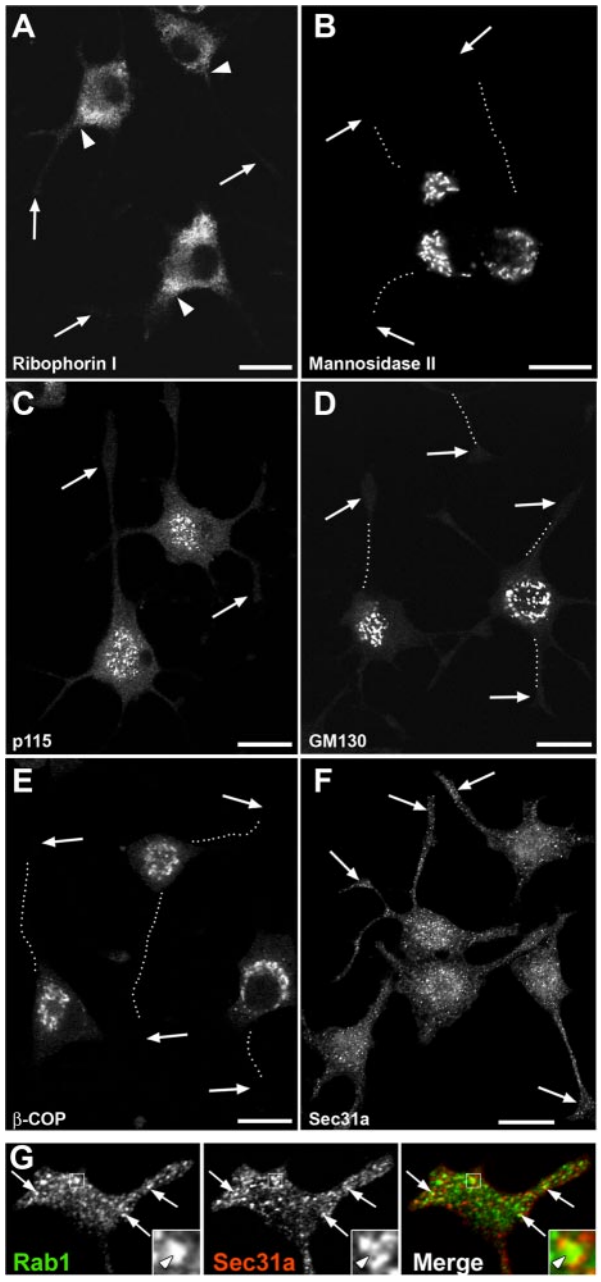

Figure 2. Distribution of early secretory compartments in polarized PC12 cells. (A–F) PC12 cells (48-h NGF) were stained with antibodies against RER (A) and Golgi (B) markers, p115 (C), GM130 (D), and the β-COP and Sec31a subunits of COPI and COPII coats (E and F, respectively). Note the exclusion of all markers from the neurites, except for ribophorin I (RER) that is present in their neck regions (A, arrowheads), and Sec31a, a marker for ERES, that is found throughout the cell body and the neurites. Arrows indicate growth cones and the dotted lines highlight the paths of the neurites. Bars, 20 μm. (G) Close association of the Rab1-positive IC elements and ERES in the growth cones (arrows). The inset shows an IC element surrounded by three ERES.

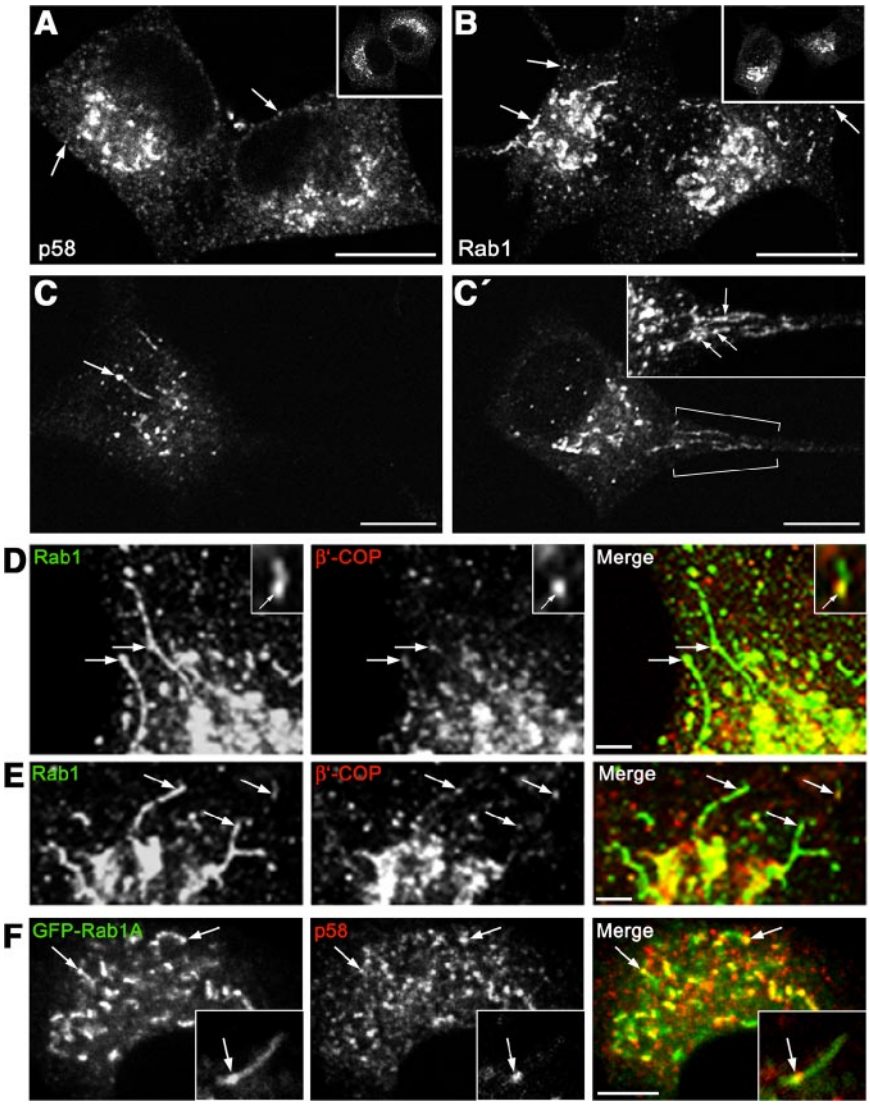

Figure 3. Expansion of the IC in NGF-treated cells. (A and B) Localization of p58 (A) and Rab1 (B) in control and NGF-treated (24 h) cells. Compared with control cells (insets), more widespread distribution of the IC elements (arrows) is seen in the differentiating cells. (C and C′) Two confocal sections from a cell (24-h NGF) stained for Rab1 (see Supplemental Movie 1). Note the globular and tubular domains of the IC element in C (arrow) and the formation of a reticulum in the neck region of the neurite (C′, brackets; inset). (D and E) Double staining for endogenous Rab1 and β′-COP shows that the IC tubules (arrows) mostly lack COPI but can be continuous with COPI-positive globular domains (D, inset). (F and Inset) GFP-Rab1A and p58 colocalize in globular IC domains (arrows), whereas the Rab1-positive tubules are devoid of p58 (inset). Bar, 5 μm. Bars, 10 μm (A and B), 10 μm (C and C′), and 2 μm (D and E).

Barr and Short, 2003) were localized to membranes in the Golgi region as well as peripheral IC structures within the cell bodies, as described in other cell types (Alvarez *et al*., 1999; Marra *et al*., 2001). Interestingly, when different antibodies were used, both were consistently found to be excluded from the neurites (Figure 2, C and D).

Antibodies against β-COP, a subunit of COPI coats that predominantly associate with IC and *cis*-Golgi membranes (Klumperman, 2000; Sannerud *et al*., 2003), revealed predominant localization of these membrane-bound coats to the cell bodies, with negligible signal in the neurites (Figure 2E). By contrast, antibodies against mSec13 and Sec31a (Figure 2F), two COPII components (Antonny and Schekman, 2001), highlighted the punctate ERES and showed their presence in the neurites, as recently reported for hippocampal neurons (Horton and Ehlers, 2003, Aridor *et al*., 2004). Double localization of endogenous Rab1 and Sec31a showed that many of the IC elements and ERES closely associate within the growth cones (Figure 2G). Examination of cells at different times after NGF addition showed that the redistribution of ERES occurs in parallel with neurite growth (our unpublished data).

Expansion of the IC during Neurite Outgrowth

The redistribution of Rab1-containing IC elements to the developing neurites indicated that differentiation of PC12 cells is accompanied by considerable reorganization of this compartment. It has been reported that NGF treatment of PC12 cells results in approximately sixfold induction of Rab1B mRNA (Zhu *et al*., 2002), and we measured a corresponding up to fourfold increase in Rab1 protein levels (Sannerud and Saraste, unpublished data). Localization of p58 and Rab1 in PC12 cells at 12–24 h after NGF addition, before major redistribution of Rab1 to the neurites (Figure 1C), indicated that considerable expansion of the IC indeed takes place. Whereas the IC elements in control cells were concentrated in the Golgi region (Figure 3, A and B, insets), in NGF-treated cells they were spread throughout the cytoplasm, including its cortical regions (Figure 3, A and B). Interestingly, proliferation of Rab1-positive tubules occurred in the differentiating cells (Figure 3, B and C), and analysis of serial confocal sections revealed the formation of tubular networks in the neck regions of the neurites (Figure 3, C′ and inset; see Supplemental Movie 1).

The IC Consists of Compositionally Distinct Domains

In contrast to Rab1, p58 was not detected in tubular elements in the NGF-treated PC12 cells (Figure 3A). To directly compare the distributions of these two proteins, we localized endogenous p58 in the differentiating cells transiently expressing the GFP-Rab1A fusion protein (see below; Figure 7A). As shown in Figure 3F, p58 was absent from the IC tubules, but colocalized with GFP-Rab1A in the globular domains. In addition, because retrograde transport at the ER–Golgi boundary seems to involve distinct pathways that differ in their dependency of COPI coats (see Sannerud *et al*., 2003 for review), we studied the localization of these coats with respect to the Rab1 tubules that accumulate in the differentiating cells. Double-staining of cells for Rab1 and the β'-COP subunit of COPI coats indicated that the Rab1-positive IC tubules generally are devoid of these coats; however, some apparent patchy overlap was seen along the tubules (Figure 3, D and E). In addition, Rab1 and β'-COP displayed largely nonoverlapping distributions in IC elements consisting of distinct globular and tubular domains (Figure 3D, insets).

Brefeldin A Results in Transport of p58 to the Neurites

The above-mentioned results suggested that the segregation of Rab1 from p58 and COPI in the differentiating PC12 cells could result from their differential distributions within tubular and globular domains of the IC. Because the binding of COPI coats to IC membranes is inhibited by BFA (Lippincott-Schwartz *et al*., 2000), and p58 is known to interact with these coats (Hauri *et al*., 2000), we studied the effect of this inhibitor on the segregation of p58 and Rab1. When BFA was added to cells pretreated for 24 h with NGF, the p58-specific signal in the growth cones increased approximately fivefold but returned to control levels after BFA washout (Figure 4A). In contrast, the Rab1 signal was unaffected by these treatments, and gradually increased, as in control cells at 24 h after addition of NGF (Figure 4A). Confocal microscopy showed that BFA resulted in the appearance of p58 in tubular structures within the cell bodies and the neck regions of the neurites (Figure 4B) as well as partial colocalization of p58 and GFP-Rab1A in growth cones of the drug-treated cells (Figure 4C). Under the same experimental conditions, mannosidase II was not detected in the neurites (our unpublished data). These results indicate that the retention of p58 within the cell bodies involves a COPI-dependent mechanism, whereas transport of IC elements to the growth cones does not require COPI function.

Dynamics of GFP-Rab1A in Living Cells

To visualize the dynamics of Rab1-positive IC elements in living cells, we constructed a chimeric protein consisting of GFP fused to the NH_2 terminus of Rab1A (GFP-Rab1A). The localization of GFP-Rab1A in the transfected cells (HeLa, NRK, and PC12), expressing moderate levels of the fusion protein, was indistinguishable from that of endogenous Rab1, and the expression of the fusion protein did not affect the distribution of endogenous proteins of the early secretory pathway (mSec13, p58, KDEL-receptor, and mannosidase II; data not shown). Moreover, PC12 cells expressing GFP-Rab1A responded to NGF like nontransfected cells, and the fusion protein redistributed to the growth cones of the differentiating cells (see below; Figure 7A).

The dynamics of GFP-Rab1A was first studied by confocal time-lapse microscopy in nonpolarized HeLa cells (Figure 5 and Supplemental Movie 2). GFP-Rab1A associated with long tubular (apparent length 1.4–3 μm) and large globular

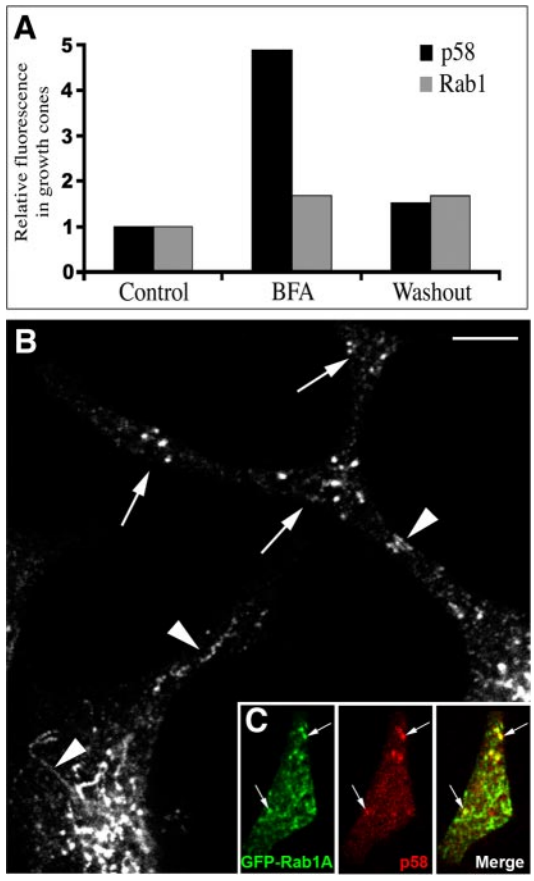

Figure 4. BFA causes redistribution of p58 to the growth cones. (A) The relative p58- and Rab1-specific signals were determined in the growth cones of NGF-treated cells at the time of BFA addition (24-h NGF; control), after BFA treatment (120 min), and after BFA washout (60 min). One of two experiments giving similar results is shown. (B) In contrast to NGF-treated control cells (Figure 2A), p58 localizes to tubular elements (arrowheads) in the BFA-treated cells and is found in the varicosities and growth cones of the neurites (arrows). (C) GFP-Rab1A and p58 (arrows) colocalize in the growth cones of transfected cells BFA-treated as in A. Bar, 5 μm (B).

structures (diameter 0.2–0.5 μm), which were found throughout the cytoplasm, including its cortical regions (Figure 5A). Although most of these elements were highly dynamic, many of the globular structures remained stationary for variable periods of time but suddenly changed their shape and became mobile (Figure 5A and Supplemental Movie 2; see also Figure 6C and Supplemental Movie 5). Staining of the cells expressing GFP-Rab1A with antibodies against mSec13 indicated that many of the globular elements localize to the vicinity of ERES (Figure 5B). Interestingly, the fluorescent signal of the stationary, globular structures fluctuated in a periodic manner (Figure 5C). The signal rises frequently followed bimodal kinetics, apparently corresponding to the recruitment of GFP-Rab1A from the cytosol, or fusion between different IC elements (Figure 5, C and F, and Supplemental Movie 3), whereas the rapid drops in signal intensity represent the conversion of the IC elements to mobile structures (Figure 5C and Supplemental Movie 3). The reappearance of the signal at the same sites (Figure 5C and Supplemental Movie 3) further indicates that these lie close to ERES, which maintain fixed positions over time (Hammond and Glick, 2000; Stephens *et al*., 2000).

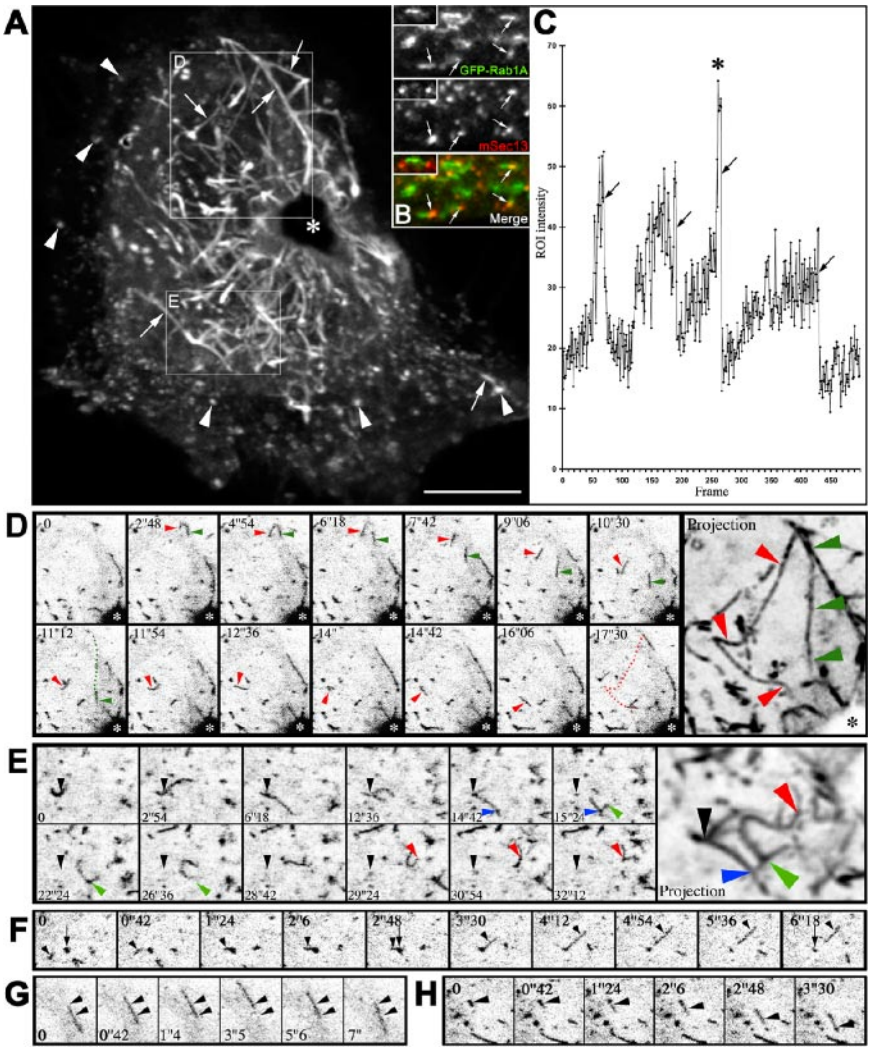

Figure 5. Dynamics of GFP-Rab1A in HeLa cells. (A) GFP-Rab1A dynamics visualized by time-lapse confocal microscopy. Projection of 100 images (frames 300–399; Supplemental Movie 2) reveals the trajectories (arrows) followed by mobile IC elements. The arrowheads indicate stationary IC elements at the periphery of the cells. The Golgi region (asterisk) looks dark in this projection. The areas shown in D and E are indicated. Bar, 10 μm. (B and Inset) Partially overlapping distributions of GFP-Rab1A and endogenous mSec13 (ERES) in the transfected HeLa cells. (C) Oscillation of the GFP signal at a peripheral site (also see Supplemental Movie 3). The asterisk indicates a rapid rise in signal intensity coinciding with fusion between two globular IC elements. (D) Distinct trajectories (red and green arrowheads) of two tubular IC elements that originate at the same site and move toward the Golgi region (frames 318–342; see Supplemental Movie 2). (E) Dynamic networks formed by tubules that bud from peripheral IC elements and merge with nearby sites (frames 359–398; see Supplemental Movie 2). The projection shows the ramified trajectories of the tubules and the branch points of the network (colored arrowheads). (F) Fusion of two IC elements, followed by budding of a narrow tubule (arrowhead) from the merged, stationary element (arrow) (frames 337–346; see Supplemental Movie 2). (G) Bidirectional movements of a tubular IC element along the same path (frames 257–267; see Supplemental Movie 2). (H) A stationary globular element assumes an elongated, tubular shape as it starts to move (frames 243–248; see Supplemental Movie 2).

Many of the GFP-Rab1A-positive tubular and globular elements moved centripetally, apparently merging with IC membranes in the Golgi region (Supplemental Movies 2 and 3; Marra *et al*., 2001). In addition, a number of the structures moved centrifugally from the Golgi area toward peripheral sites. Multiple bidirectional, long-range movements followed the same tracks, suggesting that they occur along microtubules (Figure 5, D and G, and Supplemental Movie 2). The velocities of the GFP-Rab1A-containing elements (0.8–1.7 μm/s) were similar to those reported for microtubule-based transport of pre-Golgi carriers (Lippincott-Schwarz *et al*., 2000), and nocodazole resulted in the accumulation of GFP-Rab1A in stationary structures throughout the cells (our unpublished data). Interestingly, narrow tubules were seen budding from globular IC elements and fusing with nearby IC structures (Figure 5, E and F), thus connecting peripheral IC elements that apparently reside close to ERES. Although the oscillation of the GFP-signal of these sites made it difficult to visualize them over time (Figure 5, C, E, and F), they could be identified as branch points of a dynamic network in projections of successive images (Figure 5F, projection). In addition, the globular IC elements seemed to undergo homotypic fusion (Figure 5F and Supplemental Movie 3).

For comparison, we also prepared fluorescent variants of p58 and followed their dynamics in transfected HeLa cells. In contrast to the results obtained with GFP-Rab1A, and recently reported for GFP-ERGIC-53 (Ben-Tekaya *et al*., 2005), YFP-p58 predominantly associated with relatively stationary, globular structures that were widely distributed in the cells. In cells expressing moderate levels of fluorescent p58, it was only occasionally detected in dynamic tubules interconnecting the globular IC elements (Supplemental Movie 4). Similar results were obtained with two different constructs of p58, YFP-p58P (Supplemental Movie 4) and YFP-p58N (Ying *et al*., 2002; our unpublished data).

The strong GFP signal facilitated the detection of IC elements also in the cortical regions of nonpolarized HeLa and NRK cells (Figure 5A and Supplemental Movie 2). To visualize the detailed dynamics of these peripheral elements, we used spinning disk confocal microscopy allowing fast acquisition of images. Narrow, GFP-Rab1-positive tubules were seen budding from globular IC structures and moving centrifugally to cortical cytoplasmic regions under the plasma membrane. Most of these tubules seemed to originate from IC structures located outside the Golgi region (Supplemental Movie 5). In the cell cortex these became relatively stationary, sometimes lying in parallel to the plasma membrane, or forming tubular networks (Figure 6, A–C, and Supplemental Movie 5). IC elements also moved in the opposite direction, from the cell cortex toward the perinuclear region (Supplemental Movie 5).

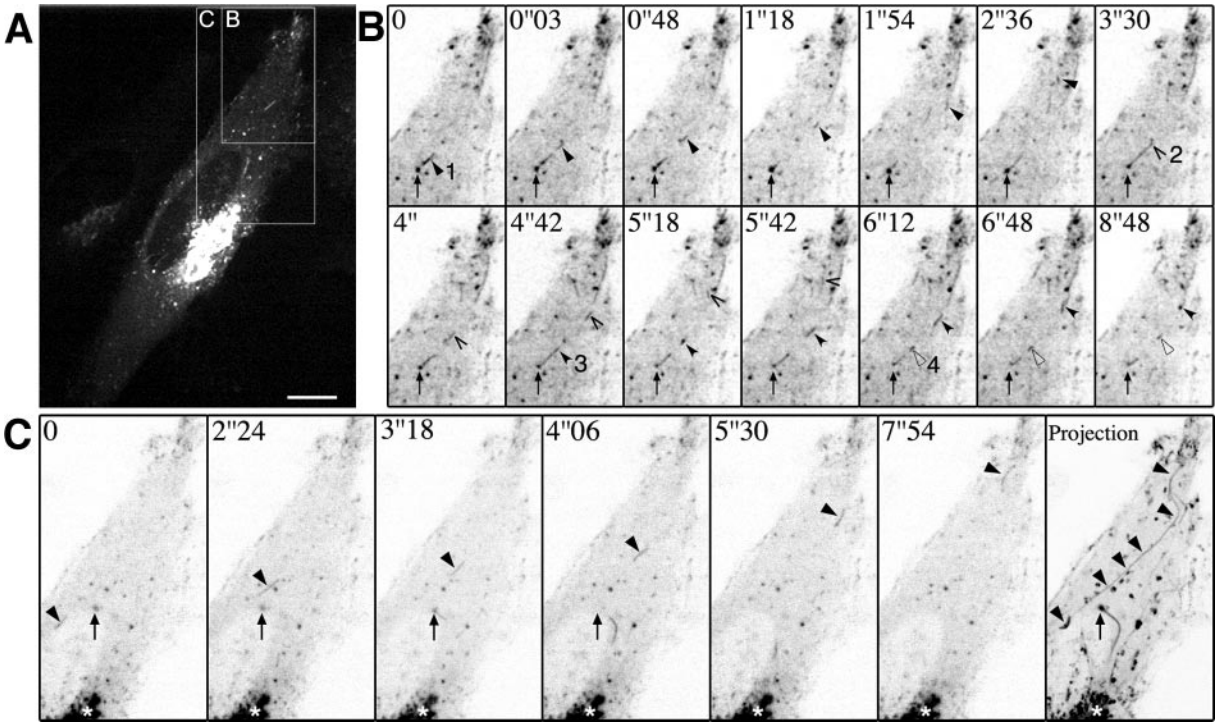

Figure 6. Centrifugal movements of IC tubules to the cell cortex. (A) An image from Supplemental Movie 5, obtained by spinning disk confocal microscopy, showing the dynamics of GFP-Rab1A in transiently transfected NRK cells. The areas shown in B and C are indicated. (B) Narrow, GFP-Rab1A-positive tubules (arrowheads 1–4) bud from the same stationary, globular structure (arrow) and move along the same track to the cell cortex (frames 774–826; see Supplemental Movie 5). (C) A tubular IC element (arrowhead) moves from a juxtanuclear site to the cell periphery (frames 572–651; see Supplemental Movie 5). The arrow denotes a globular IC element that transforms into an elongated structure as it starts to move toward the Golgi region (asterisk). Bar, 10 μm (A).

The dynamics GFP-Rab1A in the cell bodies of NGF-treated PC12 cells could not be studied with similar resolution as in the nonpolarized cells due to the small size of these cells and the expansion of IC membranes. However, the emerging picture of IC dynamics in these cells was similar to that seen in HeLa and NRK cells, including relatively stationary, globular structures, and dynamic tubules that interconnected these and also moved bidirectionally between peripheral sites and the Golgi region. In addition, narrow tubules and tubular networks were seen in the periphery of the cells, beneath the plasma membrane, and in the neck regions of the neurites (Supplemental Movie 6). Live cell imaging further showed that GFP-Rab1A-positive IC elements move bidirectionally along the neurites (Figure 7B, Supplemental Movie 6). The velocities of the movements within the neurites were relatively slow (0.2–0.3 μm/s), as compared with those recorded in HeLa cells.

Rab1-positive IC Elements Contain HMG-CoA Reductase and BiP

The unexpected transfer of Rab1A-containing IC tubules to the growth cones of polarized PC12 cells raised the question of their relationship with SER, which has been shown to be present at these sites (Luckenbill-Edds *et al*., 1979; Tooze *et al*., 1989; Krijnse-Locker *et al*., 1995). SER has mainly been characterized in highly specialized tissues, whereas its organization and dynamics in less differentiated cells is poorly understood (Baumann and Walz, 2001). Because live cell imaging showed that cells contain a consider-able pool of Rab1-positive, narrow tubules, that are largely devoid of p58, we used velocity sedimentation to separate the tubular and globular domains of the IC, which differ in both size and form. Previous analytical differential centrifugation studies showed that the IC consists of two size classes of components, most likely corresponding to the tubulo-vesicular and vacuolar structures seen by electron microscopy (Ying *et al*., 2000). Moreover, velocity sedimentation has been successfully used to separate small, Golgi-derived vesicles from large Golgi structures (Love *et al*., 1998). Using iodixanol-gradients, it was possible to separate the IC into two types of elements showing differential enrichment of Rab1 and p58 (Figure 8A). Based on their sedimentation properties and marker content we conclude that the slowly sedimenting component (67% of total membrane-bound Rab1) represents the narrow IC tubules, whereas the fast-migrating fraction (69% of total p58) is enriched in the globular (vacuolar) IC structures (Figure 8A). The minor, slowly sedimenting peak of p58 most likely corresponds to the p58-containing, small transport vesicles (Saraste and Svensson, 1991; Palokangas *et al*., 1998).

To study the distributions of ER subcompartments in these gradients, we used SPC25 (see above) and HMG-CoA reductase (HMGR; Anderson *et al*., 1983; Singer *et al*., 1988) as markers for RER and SER, respectively. In accordance with previous studies (Majoul *et al*., 1996), the RER elements were found to concentrate towards the bottom part of the gradients, partially separating from both IC fractions (Figure 8B). Interestingly, HMGR peaked at the top of the gradients where it colocalized with the slowly sedimenting IC elements enriched in Rab1. The strict colocalization of HMGR and Rab1 was not affected by changing the steepness of the gradient (our unpublished data).

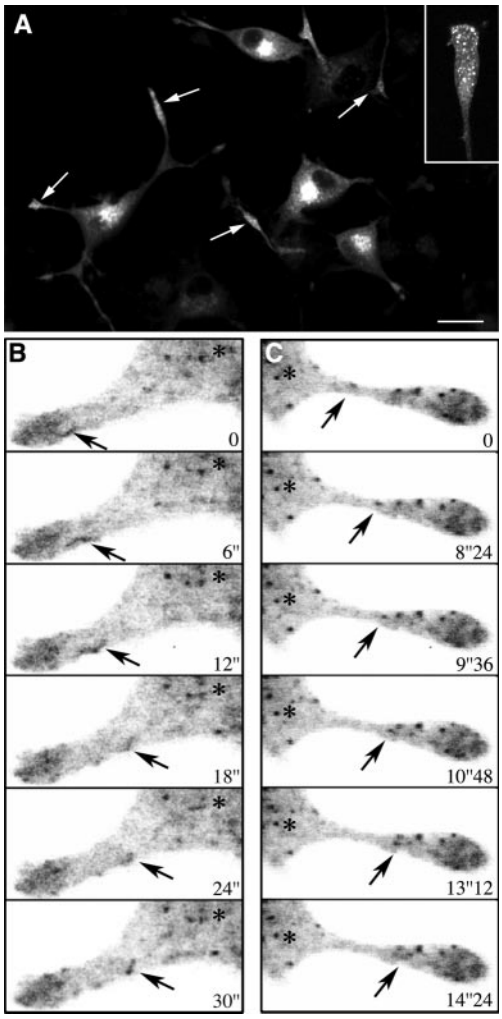

Figure 7. Bidirectional movements GFP-Rab1A in the neurites of PC12 cells. (A and Inset) GFP-Rab1A, like endogenous Rab1, is redistributed to the growth cones (arrows) of the NGF-treated cells. (B and C) Bidirectional dynamics of IC elements in the neurites recorded by time-lapse confocal microscopy (see Supplemental Movie 6). (B) A tubular IC element (arrow) moves from the growth cone toward the cell body. (C) An IC element (arrow) moving from the neck region of the neurite toward the growth cone. Asterisks indicate the cell body. Bar, 20 μm (A).

Because the antibody against HMGR was not applicable for the detection of the protein by immunocytochemistry, we compared the localization of Rab1 with that of BiP, a lumenal ER protein that has been previously shown to reside in the SER compartment present in the extensions and growth cones of neuronlike cells (Tooze *et al*., 1989). Interestingly, partial colocalization of the two proteins was observed both in the growth cones (Figure 8D, top) and along the extensions (Figure 8D, bottom) of polarized PC12 cells. In addition, a large pool of (~40%) of BiP cosedimented with the slowly migrating, Rab1-enriched IC elements in the velocity gradients (our unpublished data).

DISCUSSION

We have studied here the organization and dynamics of the IC in different polarized and nonpolarized cell types and obtained results that reveal an unexpected topological and functional complexity of this membrane system. These results are schematically summarized in Figure 9. We propose that the IC consists of two morphologically distinct (light microscopically distinguishable), globular and tubular subdomains that also differ in their composition and dynamics. Partial segregation of these domains seemed to take place in polarized PC12 cells, indicating that they have different functions. We suggest that the "globular" domain of the IC (Figure 9) operates in ER-to-Golgi transport. Accordingly, it is enriched in newly synthesized cargo proteins (Presley *et al*., 1997; Scales *et al*., 1997; Palokangas *et al*., 1998), COPI coats, and the cargo receptor p58/ERGIC-53 that interacts with these coats (Hauri *et al*., 2000). This domain most likely corresponds to (or includes) the large, pleiomorphic elements that by immunoelectron microscopy have been shown to contain p58 (Saraste and Svensson; 1991) and membrane-bound or secretory cargo (Saraste and Kuismanen, 1984; Horstmann *et al*., 2002; Mironov *et al*., 2003). It is further divided into COPI-coated and uncoated membrane regions that may have distinct functions in bidirectional (antero- and retrograde) ER-to-Golgi trafficking (Martinez-Menarguez *et al*., 1999, Shima *et al*., 1999).

The tubular subcompartment of the IC is defined by Rab1 (Figure 9), which according to the present results is enriched in this domain (Figure 8). It was first described by confocal microscopy in cells in which transport between the ER and Golgi was arrested at reduced temperature (15°C) or by blocking organelle acidification (Palokangas *et al*., 1998). Interestingly, the Rab1-positive IC tubules accumulating in the transport-arrested cells were largely devoid of anterograde cargo, suggesting that they function in a retrograde pathway (Palokangas *et al*., 1998; Sannerud *et al*., 2003). Here, we show that NGF-induced differentiation of PC12 cells leads to proliferation of this domain and its transfer to the developing neurites (Figure 9). In addition, imaging of GFP-Rab1A in living cells provided evidence that these tubules constitute a dynamic pathway that interconnects peripheral and central IC elements and also extends from the IC toward cortical regions of the cell (Figure 9). It is possible that cells contain different populations of Rab1-containing tubules that differ in their composition depending on their cellular localization (e.g., *cis*-Golgi region versus cell periphery).

The effector molecules that interact with Rab1 in the narrow IC tubules remain to be identified. Rab1 may function during the formation of the tubules, for example by regulating the recruitment of specific structural components or motors to these membranes, or in their fusion with other IC elements. As suggested in Figure 9, it is possible that COPI (Lippincott-Schwartz *et al*., 2000; Alvarez *et al*., 2003) and Rab1 play key roles in the organization of the IC into its subdomains. The function of Rab1 could also be related to the long-distance movement of the tubules. Recently, MICAL proteins were identified as novel Rab1-interacting proteins, providing a possible functional link with the cytoskeleton (Fischer *et al*., 2005).

In addition to the tubular IC elements, Rab1 is also detected in the globular IC domain (Figure 9; Palokangas *et al*., 1998), most likely corresponding to the vacuolar structures seen by electron microscopy (Saraste *et al*., 1995). Therefore, visualization of GFP-Rab1A in living cells provided a more comprehensive picture of IC dynamics than has been obtained thus far. These experiments showed that the narrow IC tubules are highly dynamic. Moreover, the globular IC elements, apparently residing in the vicinity of ERES, could remain stationary for variable periods of time, but suddenly assumed an elongated shape and became mobile. Treatment

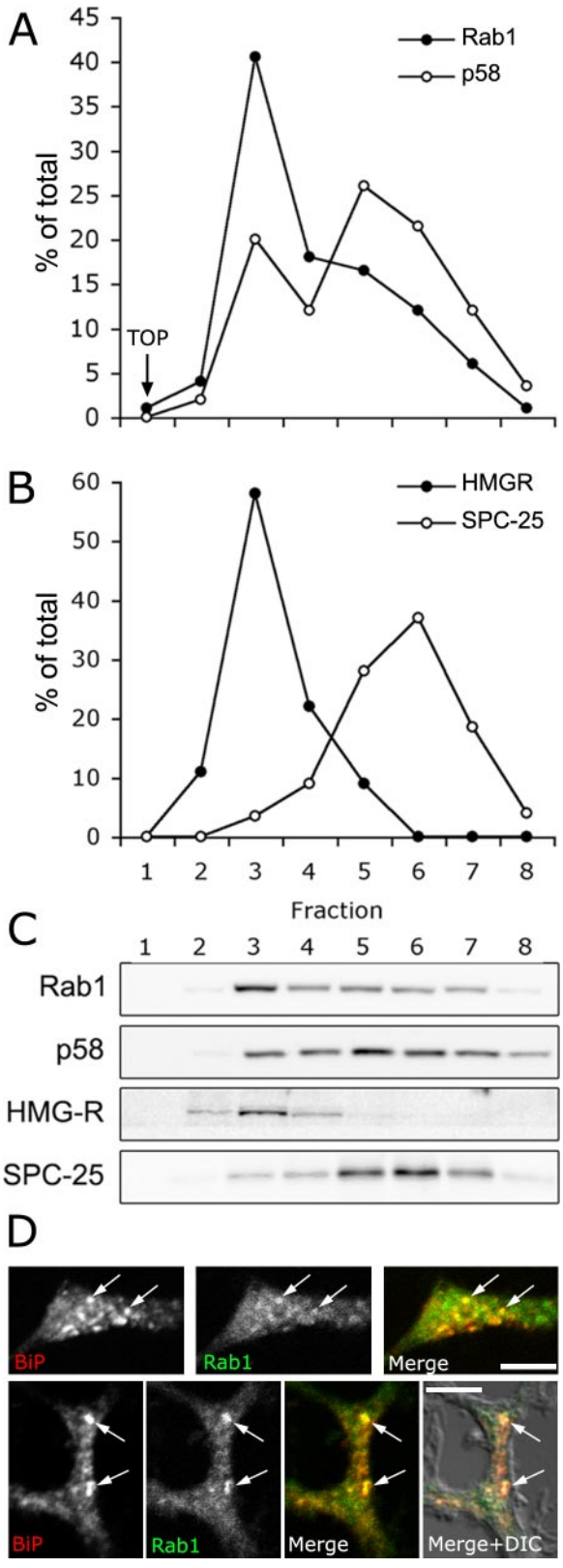

Figure 8. Localization of HMGR and BiP to Rab1-positive IC elements. (A and B) A 3000 × *g* supernatant prepared from PC12 cells was subjected to velocity sedimentation in a 5–25% iodixanol gradient, and the gradient fractions were analyzed by immunoblotting with antibodies against Rab1 and p58 (IC), HMGR (SER) and SPC-25 (RER). The distributions of the four proteins (A and B) are representative for three (Rab1, p58, and HMGR) or two experiments (SPC25). The three bottom fractions were devoid of immunoreactive material and are not shown. Note the separation of the IC elements into slow- and fast-sedimenting components, enriched in Rab1 and p58, respectively, and the colocalization of HMGR with the IC elements enriched in Rab1. (C) Corresponding immunoblots for the four proteins are shown. (D) Partially overlapping distributions of Rab1 and BiP in the neurites of PC12 cells. The arrows indicate colocalization of the two proteins in the growth cones (top) and along the extensions (bottom) of the NGF-treated cells. Bars, 5 μm.

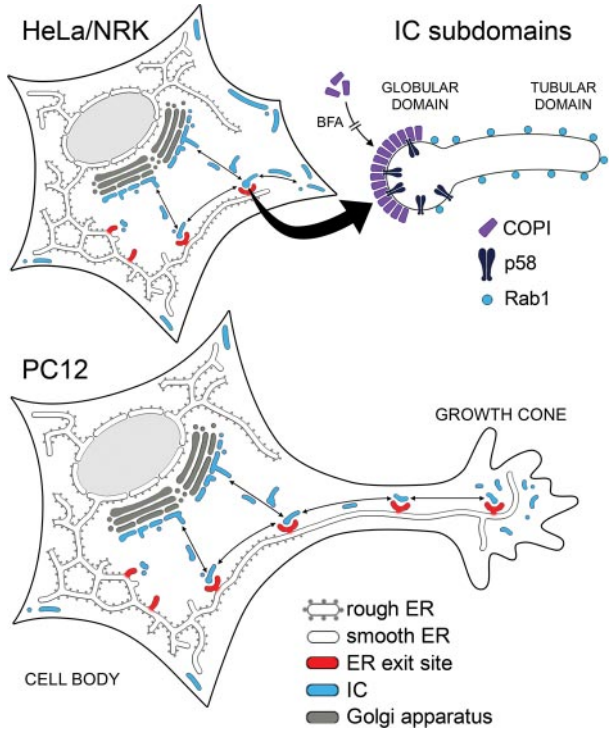

Figure 9. Dynamic organization of the IC in nonpolarized and polarized cells. Top left, schematic model of the dynamics and topology of the IC elements in nonpolarized HeLa and NRK cells. In addition to mediating two-way traffic between ER exit sites (ERES) and the *cis*-Golgi region, dynamic IC elements also interconnect different ERES and move centrifugally to cortical regions of the cytoplasm where they become more stationary. Top right, the IC consists of compositionally distinct globular and tubular domains. The globular "anterograde cargo domain" contains p58, which associates with BFA-sensitive COPI coats, whereas the tubular domain is specifically enriched in Rab1. Bottom, the Rab1-containing IC tubules move to the neurites and growth cones of differentiating PC12 cells, whereas p58/COPI-positive IC elements, like RER and Golgi membranes, remain in the cell body. However, disassembly of the COPI coats by BFA results in missorting of p58 to the tubular IC domain and its transport to the neurites. ERES also move to the neurites and their growth cones, where they together with the dynamic Rab1-containing IC elements are proposed to give rise to a smooth membrane network (SER) that in highly differentiated cells may become more stationary and establish stable connections with membranes in the cell body.

of cells with nocodazole inhibited both types of movements. Moreover, coalignment of the p58- and Rab1-positive IC elements with microtubules (Marie and Saraste, unpublished data) supports the conclusion that the bidirectional, long-range movements of these membranes take place along microtubule tracks. Live cell imaging also demonstrated the

dynamic continuity of the two IC subdomains by showing the budding and detachment of the narrow tubules from the globular IC domains. Functional evidence for this dynamic continuity was obtained when polarized PC12 cells were treated with BFA, which blocks COPI binding to IC membranes. Under these conditions, p58 occurred in tubular elements and was transported to the growth cones of the neurites, indicating that it is missorted to the IC tubules (Figure 9). Similar missorting, because high overexpression of the protein, could explain the recently reported appearance of GFP-ERGIC-53 in dynamic tubular structures (Ben-Tekaya *et al*., 2005).

The exclusion of RER and Golgi membranes as well as the Rab1 effectors p115 and GM130 from the neurites support the conclusion that the Rab1-containing tubules at these sites have functions that are not directly related to ER-to-Golgi trafficking. Interestingly, our results suggest that the function of this IC domain is related to the biogenesis and dynamics of SER. Namely, the neurites of differentiating cultured cells (Luckenbill-Edds *et al*., 1979; Tooze *et al*., 1989), like the axons and dendrites of neurons, contain SER elements that store and release Ca^{2+}, and are important for neurite formation and the function of the growth cones (Berridge, 1998). Recent studies have shown that the IC, including its tubular subdomain, contain ER Ca^{2+}-ATPase and calreticulin (Zuber *et al*., 2001; Ying *et al*., 2002; Sannerud, Berger Hansen, and Saraste, unpublished data), indicating their compositional similarity with SER. As depicted in Figure 9, the SER in the neurites may be continuous with the ER network of the cell body (Lindsey and Ellisman, 1985; Terasaki *et al*., 1994). However, recent studies have shown bidirectional, microtubule-based movements of Ca^{2+}-releasable SER elements in the dendrites of hippocampal neurons (Bannai *et al*., 2004). Imaging of GFP-Rab1A in living cells revealed that the IC tubules also share topological features with the SER elements, which often closely associate with the plasma membrane (Blaustein and Golovina, 2001).

We also show here that HMG-CoA reductase, a SER marker (Anderson *et al*., 1983; Singer *et al*., 1988), colocalizes with the Rab1-containing IC elements, supporting the idea that these represent the same membrane structures. Because HMGR is the key enzyme of cellular cholesterol synthesis, these results further suggest that the dynamic IC tubules participate in biosynthetic transport of cholesterol to the plasma membrane. The bulk of newly synthesized cholesterol en route to the plasma membrane follows a low-temperature (15°C)–sensitive, but BFA-insensitive pathway, which thus is distinct from the transport route followed by viral glycoproteins (Urbani and Simoni, 1990; Heino *et al*., 2000). This apparent Golgi-bypass route is inhibited by microtubule polymerization similarly as the classical secretory pathway (Heino *et al*., 2000). The function of IC tubules in cholesterol transport does not require their direct fusion with the plasma membrane, because the intracellular transport of cholesterol also can involve nonvesicular transfer between closely opposed ER and plasma membranes (Liscum and Munn, 1999; Baumann *et al*., 2005).

Neurite outgrowth requires a considerable increase in the synthesis of membrane components to sustain the massive expansion of the plasma membrane. Interestingly, the formation of neurites is unaffected in PC12 cell clones that lack the post-Golgi machinery of regulated secretion. By contrast, it is blocked by antisense oligonucleotides against Rab-GDIα, indicating that it involves functional Rab protein(s) other than those required for the regulated post-Golgi route (Leoni *et al*., 1999). An intriguing possibility is that the Rab1-mediated Golgi bypass pathway described here delivers certain membrane components, such as cholesterol, to the neurites and their growth cones. It could also participate in the reorganization of the secretory apparatus that takes place in developing neurons (Horton and Ehlers, 2003; Aridor et al., 2004).

In summary, the model presented in Figure 9 proposes that the two functionally distinct IC domains constitute an interconnected, highly dynamic, but at the same time stable membrane system at the ER–Golgi boundary. Our results also suggest that Rab1 has multiple functions within this dynamic IC network that involve its interaction with still unidentified effectors. Accordingly, we provide evidence for a bidirectional pathway, mediated by Rab1-containing IC elements, that connects the IC with peripheral regions of the cell, and corresponds to the dynamics of SER. Possible cargo proteins that use this novel pathway remain to be identified.

ACKNOWLEDGMENTS

We are grateful to Bodil Berger Hansen, Anita Koldingsnes, and Annick Boulet for expert technical assistance. We thank Eivind Rødahl for the PC12 cell subclone, Tommy Nilsson for the GST-Rab1A construct, and Leif Oftedal and Svend Davanger for rat hippocampal neurons. Gert Greibich, Stephen High, Kelley Moremen, Nobuhiro Nakamura, Tom Rapoport, Elizabeth Sztul, Bor Luen Tang, Wanjin Hong, and Felix Wieland generously provided antibodies. We also thank Hans-Hermann Gerdes, Volker Gerke, and Gilles Travé for helpful discussions and constructive comments on the manuscript. This study was supported by the Norwegian Cancer Society, the Novo Nordic Foundation, and the Research Council of Norway (Aurora Programme and the National Programme for Research in Functional Genomics).

REFERENCES

Allan, B. B., Moyer, B. D., and Balch, W. E. (2000). Rab1 recruitment of p115 into a *cis*-SNARE complex: programming budding COPII vesicles for fusion. Science *289*, 444–448.

Alvarez, C., Fujita, H., Hubbard, A., and Sztul, E. (1999). ER to Golgi transport: requirement for p115 at a pre-Golgi VTC stage. J. Cell Biol. *147*, 1205–1222.

Alvarez, C., Garcia-Mata, R., Brandon, E., and Sztul, E. (2003). COPI recruitment is modulated by a Rab1b-dependent mechanism. Mol. Biol. Cell *14*, 2116–2127.

Anderson, R., Orci, L., Brown, M. S., Garcia-Segura, L. M., and Goldstein, J. L. (1983). Ultrastructural analysis of the crystalloid endoplasmic reticulum in UT-1 cells and its disappearance in response to cholesterol. J. Cell Sci. *63*, 1–20.

Antonny, B., and Schekman, R. (2001). ER export: public transportation by the COPII coach. Curr. Opin. Cell Biol. *13*, 438–443.

Aridor, M., Guzik, A. K., Bielli, A., and Fish, K. N. (2004). Endoplasmic reticulum export site formation and function in dendrites. J. Neurosci. *24*, 3770–3776.

Bannai, H., Inoue, T., Nakayama, T., Hattori, M., and Mikoshiba, K. (2004). Kinesin dependent, rapid, bidirectional transport of ER sub-compartment in dendrites of hippocampal neurons. J. Cell Sci. *117*, 163–175.

Barr, F. A., and Short, B. (2003). Golgins in the structure and dynamics of the Golgi apparatus. Curr. Opin. Cell Biol. *15*, 405–413.

Baumann, O., and Walz, B. (2001). Endoplasmic reticulum of animal cells and its organization into structural and functional domains. Int. Rev. Cytol. *205*, 149–214.

Baumann, N. A., Sullivan, D. P., Ohvo-Rekilä, H., Simonot, C., Pottekat, A., Klaassen, Z., Beh, C. T., and Menon, A. K. (2005). Transport of newly synthesized cholesterol to the sterol-rich plasma membrane occurs via non-vesicular equilibration. Biochemistry *44*, 5816–5826.

Ben-Tekaya, H., Miura, K., Pepperkok, R., and Hauri, H.-P. (2005). Live imaging of bidirectional traffic from the ERGIC. J. Cell Sci. *118*, 357–367.

Berridge, M. J. (1998). Neuronal calcium signaling. Neuron *21*, 13–26.

Blaustein, M. P., and Golovina, V. A. (2001). Structural complexity and functional diversity of endoplasmic reticulum Ca^{2+} stores. Trends Neurosci. *24*, 602–608.

Cox, J. S., Chapman, R. E., and Walter, P. (1997). The unfolded protein response coordinates the production of endoplasmic reticulum protein and endoplasmic reticulum membrane. Mol. Biol. Cell *8*, 1805–1814.

Fischer, J., Weide, T., and Barnekow, A. (2005). The MICAL proteins and Rab 1, a possible link to the cytoskeleton. Biochem. Biophys. Res. Com. *328*, 415–423.

Futerman, A. H., and Banker, G. A. (1996). The economics of neurite outgrowth - the addition of new membrane to growing axons. Trends Neurosci. *19*, 144–149.

Greene, L. A., and Tischler, A. S. (1976). Establishment of a noradrenergic clonal line of rat adrenal pheochromocytoma cells which respond to nerve growth factor. Proc. Natl. Acad. Sci. USA *73*, 2424–2428.

Griffiths, G., Ericsson, M., Krijnse-Locker, J., Nilsson, T., Goud, B., Soling, H. D., Tang, B. L., Wong, S. H., and Hong, W. (1994). Localization of the Lys, Asp, Glu, Leu tetra-peptide receptor to the Golgi complex and the intermediate compartment in mammalian cells. J. Cell Biol. *127*, 1557–1574.

Hammond, A. T., and Glick, B. S. (2000). Dynamics of transitional endoplasmic reticulum sites in vertebrate cells. Mol. Biol. Cell *11*, 3013–3030.

Hauri, H. P., Kappeler, F., Andersson, H., and Appenzeller, C. (2000). ERGIC-53 and traffic in the secretory pathway. J. Cell Sci. *113*, 587–596.

Heino, S., Lusa, S., Somerharju, P., Ehnholm, C., Olkkonen, V. M., and Ikonen, E. (2000). Dissecting the role of the Golgi complex and lipid rafts in biosynthetic transport of cholesterol to the cell surface. Proc. Natl. Acad. Sci. USA *97*, 8375–8380.

Hickey, W. F., Stieber, A., Hogue-Angeletti, R., Gonatas, J., and Gonatas, N. K. (1983). Nerve growth factor induced changes in the Golgi apparatus of PC-12 rat pheochromo-cytoma cells as studied by ligand endocytosis, cytochemical and morphometric methods. J. Neurocytol. *12*, 751–766.

Horstmann, H., Ng, C. P., Tang, B. L., and Hong, W. (2002). Ultrastructural characterization of endoplasmic reticulum-Golgi transport containers (EGTC). J. Cell Sci. *115*, 4263–4273.

Horton, A. C., and Ehlers, M. D. (2003). Dual modes of endoplasmic reticulum-to-Golgi transport in dendrites revealed by live-cell imaging. J. Neurosci. *23*, 6188–6199.

Kelly, R. B., and Grote, E. (1993). Protein targeting in the neuron. Annu. Rev. Neurosci. *16*, 95–127.

Klumperman, J. (2000). Transport between ER and Golgi. Curr. Opin. Cell Biol. *12*, 445–449.

Krijnse-Locker, J., Parton, R. G., Fuller, S. D., Griffiths, G., and Dotti, C. G. (1995). The organization of the endoplasmic reticulum and the intermediate compartment in cultured rat hippocampal neurons. Mol. Biol. Cell *6*, 1315–1332.

Kuismanen, E., and Saraste, J. (1989). Low temperature-induced transport blocks as tools to manipulate membrane traffic. Methods Cell Biol. *32*, 257–274.

Lahtinen, U., Dahllof, B., and Saraste, J. (1992). Characterization of a 58 kDa cis-Golgi protein in pancreatic exocrine cells. J. Cell Sci. *103*, 321–333.

Lahtinen, U., Hellman, U., Wernstedt, C., Saraste, J., and Pettersson, R. F. (1996). Molecular cloning and expression of a 58-kDa cis-Golgi and intermediate compartment protein. J. Biol. Chem. *271*, 4031–4037.

Leoni, C., Menegon, A., Benfenati, F., Toniolo, D., Pennuto, M., and Valtorta, F. (1999). Neurite extension occurs in the absence of regulated exocytosis in PC12 subclones. Mol. Biol. Cell *10*, 2919–2931.

Lindsey, J. D., and Ellisman, M. H. (1985). The neuronal endomembrane system. III. The origins of the axoplasmic reticulum and discrete axonal cisternae at the axon hillock. J. Neurosci. *5*, 3135–3144.

Lippincott-Schwartz, J., Roberts, T. H., and Hirschberg, K. (2000). Secretory protein trafficking and organelle dynamics in living cells. Annu. Rev. Cell Dev. Biol. *16*, 557–589.

Liscum, L., and Munn, N. J. (1999). Intracellular cholesterol transport. Biochim. Biophys. Acta *1438*, 19–37.

Love, H. D., Lin, C. C., Short, C. S., and Ostermann, J. (1998). Isolation of functional Golgi-derived vesicles with a possible role in retrograde transport. J. Cell Biol. *140*, 541–551.

Luckenbill-Edds, L., Van Horn, C., and Greene, L. A. (1979). Fine structure of initial outgrowth of processes induced in a pheochromocytoma cell line (PC12) by nerve growth factor. J. Neurocytol. *8*, 493–511.

Majoul, I. V., Bastiaens, P., and Soling, H. D. (1996). Transport of an external Lys-Asp-Glu-Leu (KDEL) protein from the plasma membrane to the endoplasmic reticulum: studies with cholera toxin in Vero cells. J. Cell Biol. *133*, 777–789.

Marra, P., Maffucci, T., Daniele, T., Tullio, G. D., Ikehara, Y., Chan, E. K., Luini, A., Beznoussenko, G., Mironov, A., and De Matteis, M. A. (2001). The GM130 and GRASP65 Golgi proteins cycle through and define a subdomain of the intermediate compartment. Nat. Cell Biol. *3*, 1101–1113.

Martinez-Menarguez, J. A., Geuze, H. J., Slot, J. W., and Klumperman, J. (1999). Vesicular tubular clusters between the ER and Golgi mediate concentration of soluble secretory proteins by exclusion from COPI-coated vesicles. Cell *98*, 81–90.

Mironov, A. A., *et al*. (2003). ER-to-Golgi carriers arise through direct *en bloc* protrusion and multistage maturation of specialized ER exit domains. Dev. Cell *5*, 583–594.

Mizuno, M., and Singer, S. J. (1994). A possible role of stable microtubules in intracellular transport from the endoplasmic reticulum to the Golgi apparatus. J. Cell Sci. *107*, 1321–1331.

Moyer, B. D., Allan, B. B., and Balch, W. E. (2001). Rab1 interaction with a GM130 effector complex regulates COPII vesicle *cis*-Golgi tethering. Traffic *2*, 268–276.

Nohturfft, A., Yabe, D., Goldstein, J. L., Brown, M. S., and Espenshade, P. J. (2000). Regulated step in cholesterol feedback localized to budding of SCAP from ER membranes. Cell *102*, 315–323.

Nunnari, J., and Walter, P. (1996). Regulation of organelle biogenesis. Cell *84*, 389–394.

Palokangas, H., Ying, M., Väänänen, K., and Saraste, J. (1998). Retrograde transport from the pre-Golgi intermediate compartment and the Golgi complex is affected by the vacuolar H^+-ATPase inhibitor bafilomycin A1. Mol. Biol. Cell *9*, 3561–3578.

Pfeffer, S. (2003). Membrane domains in the secretory and endocytic pathways. Cell *112*, 507–517.

Plutner, H., Cox, A. D., Pind, S., Khosravi-Far, R., Bourne, J. R., Schwaninger, R., Der, C. J., and Balch, W. E. (1991). Rab1b regulates vesicular transport between the endoplasmic reticulum and successive Golgi compartments. J. Cell Biol. *115*, 31–43.

Presley, J. F., Cole, N. B., Schroer, T. A., Hirschberg, K., Zaal, K. J., and Lippincott-Schwartz, J. (1997). ER-to-Golgi transport visualized in living cells. Nature *389*, 81–85.

Raposo, G., Kleijmeer, M. J., Posthuma, G., Slot, J. W., and Geuze, H. J. (1997). Immunogold labeling of ultrathin cryosections: application in immunology. In: Handbook of Experimental Immunology, ed. D. M. Weir, Cambridge, MA: Blackwell Science, 1–11.

Raposo, G., van Santen, H. M., Leijendekker, R., Geuze, H. J., and Ploegh, H. L. (1995). Misfolded major histocompatibility complex class I molecules accumulate in an expanded ER-Golgi intermediate compartment. J. Cell Biol. *131*, 1403–1419.

Sannerud, R., Saraste, J., and Goud, B. (2003). Retrograde traffic in the biosynthetic-secretory route: pathways and machinery. Curr. Opin. Cell Biol. *15*, 438–445.

Saraste, J., and Kuismanen, E. (1984). Pre- and post-Golgi vacuoles operate in the transport of Semliki Forest virus membrane glycoproteins to the cell surface. Cell *38*, 535–549.

Saraste, J., and Kuismanen, E. (1992). Pathways of protein sorting and membrane traffic between the rough endoplasmic reticulum and the Golgi complex. Semin. Cell Biol. *3*, 343–355.

Saraste, J., Lahtinen, U., and Goud, B. (1995). Localization of the small GTP-binding protein rab1p to early compartments of the secretory pathway. J. Cell Sci. *108*, 1541–1552.

Saraste, J., and Svensson, K. (1991). Distribution of the intermediate elements operating in ER to Golgi transport. J. Cell Sci. *100*, 415–430.

Scales, S. J., Pepperkok, R., and Kreis, T. E. (1997). Visualization of ER-to-Golgi transport in living cells reveals a sequential mode of action for COPII and COPI. Cell *90*, 1137–1148.

Sesso, A., de Faria, F. P., Iwamura, E. S., and Correa, H. (1994). A three-dimensional reconstruction study of the rough ER-Golgi interface in serial thin sections of the pancreatic acinar cell of the rat. J. Cell Sci. *107*, 517–528.

Shima, D. T., Scales, S. J., Kreis, T. E., and Pepperkok, R. (1999). Segregation of COPI-rich and anterograde-cargo-rich domains in endoplasmic-reticulum-to-Golgi transport complexes. Curr. Biol. *9*, 821–824.

Singer, I. I., Scott, S., Kazazis, D. M., and Huff, J. W. (1988). Lovastatin, an inhibitor of cholesterol synthesis, induces hydroxymethylglytaryl-coenzyme A reductase directly on membranes of expanded smooth endoplasmic reticulum in rat hepatocytes. Proc. Natl. Acad. Sci. USA *85*, 5264–5268.

Stephens, D. J., Lin-Marq, N., Pagano, A., Pepperkok, R., and Paccaud, J. (2000). COPI-coated ER-to-Golgi transport complexes segregate from COPII in close proximity to ER exit sites. J. Cell Sci. *113*, 2177–2185.

Tang, B. L., Low, S. H., Hauri, H. P., and Hong, W. (1995). Segregation of ERGIC-53 and the mammalian KDEL receptor upon exit from the 15°C compartment. Eur. J. Cell Biol. *68*, 398–410.

Tang, B. L., Zhang, T., Low, D. Y., Wong, E. T., Horstmann, H., and Hong, W. (2000). Mammalian homologues of yeast sec31p. An ubiquitously expressed form is localized to endoplasmic reticulum (ER) exit sites and is essential for ER-Golgi transport. J. Biol. Chem. *275*, 13597–13604.

Terasaki, M., Slater, N. T., Fein, A., Schmidek, A., and Reese, T. S. (1994). Continuous network of endoplasmic reticulum in cerebellar Purkinje neurons. Proc. Natl. Acad. Sci. USA *91*, 7510–7514.

Tisdale, E. J., Bourne, J. R., Khosravi-Far, R., Der, C. J., and Balch, W. E. (1992). GTP-binding mutants of rab1 and rab2 are potent inhibitors of vesicular transport from the endoplasmic reticulum to the Golgi complex. J. Cell Biol. *119*, 749–761.

Tooze, J., Hollinshead, M., Fuller, S. D., Tooze, S. A., and Huttner, W. B. (1989). Morphological and biochemical evidence showing neuronal properties in AtT-20 cells and their growth cones. Eur. J. Cell Biol. *49*, 259–273.

Trucco, A., *et al*. (2004). Secretory traffic triggers the formation of tubular continuities across Golgi subcompartments. Nat. Cell Biol. *6*, 1071–1081.

Urbani, L., and Simoni, R. D. (1990). Cholesterol and vesicular stomatitis virus G protein take separate routes from the endoplasmic reticulum to the plasma membrane. J. Biol. Chem. *265*, 1919–1923.

Valtorta, F., and Leoni, C. (1999). Molecular mechanisms of neurite extension. Philos. Trans. R. Soc. Lond. *354*, 387–394.

Vertel, B. M., Walters, L. M., and Mills, D. (1992). Subcompartments of the endoplasmic reticulum. Semin. Cell Biol. *3*, 325–341.

van Anken, E., Romijn, E. P., Maggioni, C., Mezghani, A., Sitia, R., Braakman, I., and Heck, A.J.R. (2003). Sequential waves of functionally related proteins are expressed when B cells prepare for antibody production. Immunity *18*, 243–253.

Warren, G., and Wickner, W. (1996). Organelle inheritance. Cell *84*, 395–400.

Watson, P., Forster, R., Palmer, K. J., Pepperkok, R., and Stephens, D. J. (2005). Coupling of ER exit to microtubules through direct interaction of COPII with dynactin. Nat. Cell Biol. *7*, 48–55.

Weide, T., Bayer, M., Koster, M., Siebrasse, J. P., Peters, R., and Barnekow, A. (2001). The Golgi matrix protein GM*130*, a specific partner of the small GTPase rab1b. EMBO Rep. *2*, 336–341.

Wiest, D. L., Burkhardt, J. K., Hester, S., Hortsch, M., Meyer, D. I., and Argon, Y. (1990). Membrane biogenesis during B cell differentiation: most endoplasmic reticulum proteins are expressed coordinately. J. Cell Biol. *110*, 1501–1511.

Wilson, C. M., Kraft, C., Duggan, C., Ismail, N., Crawshaw, S. G., and High, S. (2005). Ribophorin I associates with a subset of membrane proteins after their integration at the sec61 translocon. J. Biol. Chem. *280*, 4195–4206.

Ying, M., Flatmark, T., and Saraste, J. (2000). The p58-positive pre-Golgi intermediates consist of distinct subpopulations of particles that show differential binding of COPI and COPII coats and contain vacuolar H^+-ATPase. J. Cell Sci. *113*, 3623–3638.

Ying, M., Sannerud, R., Flatmark, T., and Saraste, J. (2002). Colocalization of Ca^{2+}-ATPase and GRP94 with p58 and the effects of thapsigargin on protein recycling suggest the participation of the pre-Golgi intermediate compartment in intracellular Ca^{2+} storage. Eur. J. Cell Biol. *81*, 469–483.

Zhu, Y., Hon, T., Ye, W., and Zhang, L. (2002). Heme deficiency interferes with the Ras-mitogen-activated protein kinase signaling pathway and expression of a subset of neuronal genes. Cell Growth Differ. *13*, 431–439.

Zuber, C., Fan, J. Y., Guhl, B., Parodi, A., Fessler, J. H., Parker, C., and Roth, J. (2001). Immunolocalization of UDP-glucose:glycoprotein glucosyltransferase indicates involvement of pre-Golgi intermediates in protein quality control. Proc. Natl. Acad. Sci. *98*, 10710–10715.

Zuber, C., Fan, J. Y., Guhl, B., and Roth, J. (2004). Misfolded proinsulin accumulates in expanded pre-Golgi intermediates and endoplasmic reticulum subdomains in pancreatic beta cells of Akita mice. FASEB J. *18*, 917–919.